ARTICLE

doi:10.1038/nature13846

Clathrin regenerates synaptic vesicles from endosomes

Shigeki Watanabe[1], Thorsten Trimbuch[2], Marcial Camacho-Pérez[2], Benjamin R. Rost[2,3], Bettina Brokowski[2], Berit Söhl-Kielczynski[2], Annegret Felies[2], M. Wayne Davis[1], Christian Rosenmund[2] & Erik M. Jorgensen[1]

Ultrafast endocytosis can retrieve a single, large endocytic vesicle as fast as 50–100 ms after synaptic vesicle fusion. However, the fate of the large endocytic vesicles is not known. Here we demonstrate that these vesicles transition to a synaptic endosome about one second after stimulation. The endosome is resolved into coated vesicles after 3 s, which in turn become small-diameter synaptic vesicles 5–6 s after stimulation. We disrupted clathrin function using RNA interference (RNAi) and found that clathrin is not required for ultrafast endocytosis but is required to generate synaptic vesicles from the endosome. Ultrafast endocytosis fails when actin polymerization is disrupted, or when neurons are stimulated at room temperature instead of physiological temperature. In the absence of ultrafast endocytosis, synaptic vesicles are retrieved directly from the plasma membrane by clathrin-mediated endocytosis. These results may explain discrepancies among published experiments concerning the role of clathrin in synaptic vesicle endocytosis.

Clathrin is thought to act at the plasma membrane of synapses to retrieve synaptic vesicle membrane and proteins. There is an extensive literature supporting this conclusion. Classic ultrastructural studies of frog neuromuscular junctions revealed the presence of clathrin coats on the plasma membrane after stimulation, suggesting that synaptic vesicles are reconstituted at the surface[1]. Biochemical purification of clathrin-coated vesicles from rat brain demonstrated that synaptic vesicle proteins co-purify with clathrin and AP2 (ref. 2), and AP2 and clathrin are sufficient to generate vesicles from purified brain lipids[3,4]. Transmembrane vesicle proteins, such as synaptotagmin[5–7] and synaptrobrevin[8,9], interact with adaptor proteins at the plasma membrane and these interactions are required for regenerating functional synaptic vesicles. These studies lend strong support to the idea that clathrin acts at the plasma membrane to regenerate functional synaptic vesicles. However, recent morphological studies[10,11] suggest that endocytosis may be much faster than previously described for clathrin-mediated endocytosis.

'Flash-and-freeze' fixation combines optogenetic stimulation with high-pressure freezing to capture events at synapses milliseconds after stimulation. Our ultrastructural studies demonstrated that endocytic pits, which lacked stereotypical clathrin coats, appeared ~50 ms after stimulation at both *Caenorhabditis elegans*[11] and mouse synapses[10]. Ultrafast endocytosis is compensatory, that is, membrane retrieval is triggered by the membrane added by fusion[10]. Under our stimulation conditions this appears to be due to multiquantal release[10], as has been previously observed at cultured hippocampal synapses[12]. The large endocytic vesicles retrieved by ultrafast endocytosis are too big to be functional synaptic vesicles—they are typically equivalent to the surface area of 4 synaptic vesicles—and the fate of these vesicles was unknown.

Here we examined events that occur up to 20 s after stimulation. We performed 'flash-and-freeze' experiments on mouse hippocampal neurons and analysed the synaptic ultrastructure blind from ~200 synaptic profiles per time point. A total of 10,514 synaptic profiles and 361 tomograms were analysed. We applied a single stimulus in the presence of 4 mM Ca^{2+} or 10 stimuli (20 Hz) in the presence of 2 mM Ca^{2+}. At physiological temperatures (34–37 °C), clathrin is not required for ultrafast endocytosis but is required to bud synaptic vesicles from synaptic endosomes (Extended Data Fig. 1). However, at room temperature (~22 °C), clathrin functions at the plasma membrane during endocytosis.

Synaptic vesicles reform from endosomes

Clathrin polyhedral coats on endocytic membranes are distinctive in electron micrographs (Fig. 1 and Extended Data Fig. 2). In our preparations, these coats are observed on pits on the cell body (Extended Data Fig. 2d) but rarely observed on the plasma membrane at synapses. To test the requirement of clathrin after stimulation, a single stimulus was applied to hippocampal cells expressing a variant of channelrhodopsin (ChetaTC)[13]. The experiments were performed in the presence of 4 mM Ca^{2+} in the external solution at 34 °C (Fig. 1) and 37 °C (Extended Data Fig. 2). After a single stimulus, endocytic pits that lack distinctive clathrin coats formed 50–100 ms after fusion (Fig. 1a, left panel; Extended Data Fig. 2a, left panel)[10]. These invaginations resolved into large vesicles about 80 nm in diameter at the lateral edges of the active zone (Fig. 1a and Extended Data Fig. 2a). The number of large endocytic vesicles adjacent to the plasma membrane peaked at 100 ms (Fig. 1d; Extended Data Fig. 2e). Thereafter, endosome-like structures began accumulating in the bouton and peaked at 1 s (Fig. 1b, d and Extended Data Fig. 2b, e). These organelles are larger in diameter (116.4 ± 2.5 nm, 8 synaptic vesicle equivalents) than the endocytic vesicles at the periphery (80.6 ± 0.7 nm; 4 synaptic vesicle equivalents; Extended Data Fig. 3a, see Methods), suggesting that the large endocytic vesicles fuse to form a synaptic endosome[14]. Tomographic reconstructions of these endosomes demonstrated that they are not connected to the plasma membrane (Extended Data Fig. 2c and Supplementary Video 1). Clathrin-like coats were visible on some of these endosomes (Fig. 1b, c and Extended Data Fig. 2b–d), and budded endosomes peaked 3 s after stimulation (Fig. 1c, d and Extended Data Fig. 2b, c, e). The decline in endosomes was accompanied by an accumulation of clathrin-coated vesicles inside the bouton at 3 s (Fig. 1d and Extended Data Fig. 2e, f). By contrast, clathrin-coated pits on the plasma membrane were only observed in 0.4% of synaptic profiles (4/907) between 1 to 10 s after stimulation (1 s (2/332); 3 s (2/345); 10 s (0/330)) (Fig. 1d and Extended Data Fig. 2e). These results suggest that clathrin does not

[1]Department of Biology and Howard Hughes Medical Institute, University of Utah, Salt Lake City, Utah 84112-0840, USA. [2]Neuroscience Research Center Charité Universitätsmedizin Berlin, Berlin 10117, Germany. [3]German Center for Neurodegenerative Diseases (DZNE), 10117 Berlin, Germany.

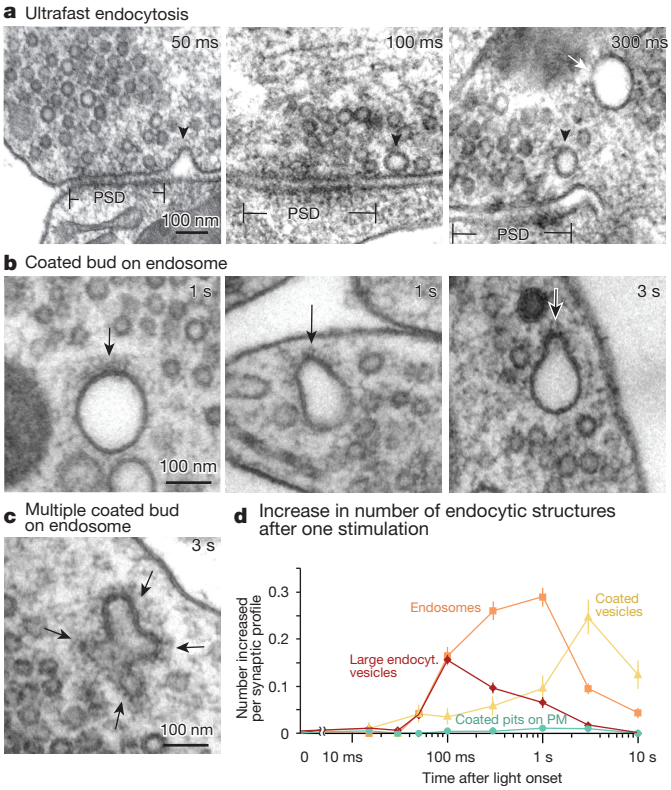

Figure 1 | Synaptic vesicles are regenerated from endosomes at 34 °C. Hippocampal synapses were stimulated once and frozen at the indicated times. **a**, Electron micrographs showing invaginations and large endocytic vesicles (black arrowheads) recovered via ultrafast endocytosis. White arrow, an endosome in the centre of the bouton. PSD, postsynaptic density. **b**, **c**, Micrographs showing single coated buds (**b**) and multiple coated buds (**c**) forming on an endosome. Black arrow, coated bud on an endosome. **d**, Increase in the number of each endocytic structure per synaptic profile after a single stimulus. Approximately 60% of synapses had endosomes in the unstimulated control; this baseline value was subtracted from endosome numbers. After stimulation, two endosomes were observed in 30% of the synapses. The prevalence of large endocytic vesicles and endosomes is followed by an increase in the number of clathrin-coated vesicles. Coated pits were rarely observed on the plasma membrane (PM). The standard error of the mean is shown in each graph. For *n* values, detailed numbers and statistical analysis, see Supplementary Table 1. Similar results were obtained from two independent cultures, and at least 178 synaptic profiles were analysed per time point (Supplementary Table 1). Endosomes are defined as vesicles larger than ~100 nm and greater than 50 nm from the active zone (see Methods and Extended Data Fig. 3).

regenerate synaptic vesicles via endocytosis at the plasma membrane but rather by budding vesicles from an endosome.

Clathrin not required for endocytosis

To test the role of clathrin in ultrafast endocytosis, we reduced expression of clathrin using RNAi[15]. Cultures were infected with lentivirus expressing a short hairpin RNA (shRNA) targeted against clathrin heavy chain mRNA, or a scrambled shRNA control. Clathrin was significantly reduced seven days after infection as determined by western blot (~80% reduction, $n = 3$; Extended Data Fig. 4a) and immunostaining (64% reduction; Extended Data Fig. 4b, d, e). Similarly, transferrin uptake was reduced by 66% (Extended Data Fig. 4c, f). Clathrin knockdown reduced release-ready vesicles but did not affect the exocytic machinery in electrophysiological recordings (Fig. 2a, Extended Data Fig. 5a–f, see Supplementary Information). Likewise, a smaller docked pool of vesicles was observed by electron microscopy, but the overall morphology of synapses was normal (Extended Data Fig. 5g, h, see Supplementary Information).

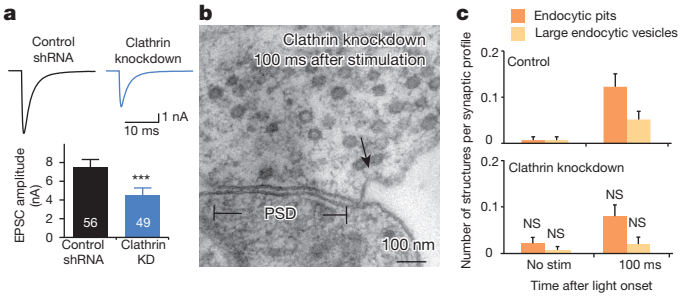

Figure 2 | Ultrafast endocytosis is clathrin-independent. **a,** Top, average traces for excitatory post-synaptic currents (EPSCs) in a control and a clathrin knockdown neuron from autaptic cultures. Bottom, mean amplitude of EPSCs. The amplitude is reduced by 41% in the knockdown cells. **b**, An electron micrograph of a synapse frozen 100 ms after stimulation. Ultrafast endocytic pit (arrow) is observed flanking the active zone. **c**, Average number of endocytic pits and large endocytic vesicles in control and clathrin knockdown neurons with or without stimulation (control 100 ms: 0.17 ± 0.03 endocytic structures per profile; knockdown 100 ms: 0.10 ± 0.03 endocytic structures per profile, $P = 0.06$). The P values are calculated against the matched time points in the control shRNA treated cells. $^{***}P < 0.001$. NS, not significant. The standard error of the mean is shown in each graph. For *n* values, detailed numbers and statistical analysis, see Supplementary Table 1.

Clathrin knockdown did not disrupt ultrafast endocytosis, which remained proportional to vesicle fusion. Following a single stimulus (34 °C, 4 mM Ca^{2+}), endocytic pits and large endocytic vesicles appeared at the edges of the active zone both in the control and clathrin knockdown cells (Fig. 2b, c). The number of endocytic pits and vesicles was decreased by 41% (Fig. 2c), closely matching the reduction in exocytosis of synaptic vesicles (Extended Data Fig. 5h). These results suggest that membrane retrieval via ultrafast endocytosis does not depend on clathrin, which is consistent with the lack of stereotypic clathrin coats on pits during ultrafast endocytosis (Fig. 1a and Extended Data Fig. 2a).

Clathrin regenerates vesicles at endosomes

To determine whether clathrin is required to resolve endosomes into synaptic vesicles, control and clathrin knockdown cells were stimulated in the presence of cationized ferritin (4 mM Ca^{2+}, 34 °C). Cationized ferritin adheres to membranes and serves as a fluid phase marker for endocytic trafficking. In control cultures 1 s after a single stimulus (Fig. 3a, b), ferritin molecules were found in endosomes but not in clathrin-coated vesicles. At 3 s, endosomes were budding and ferritin began to appear in clathrin-coated vesicles. The size of endosomes was larger than endocytic vesicles, again suggesting that endocytic vesicles carrying ferritin fuse to form synaptic endosomes (Extended Data Fig. 3b, c). Sixteen ferritin-positive endosomes were reconstructed from tomograms, none of them extended a tubule to the plasma membrane (Extended Data Fig. 6a). However, half of those endosomes were not fully contained within the 200 nm tomogram. Therefore we reconstructed 11 complete synapses by assembling serial tomograms of synapses 3 s after stimulation. None of the 17 complete end-to-end endosomes were connected to the plasma membrane (6 of which contained ferritin), suggesting that they are true intracellular organelles, not extensions of the plasma membrane (Supplementary Videos 1–5). The decline in the number of endosomes is followed by an accumulation of ferritin-positive coated vesicles and synaptic vesicles (Fig. 3b). Some clathrin-coated vesicles were observed before 3 s after stimulation (1 s, 4/149 synaptic profiles and Fig. 1d), but they did not contain ferritin molecules, suggesting that they were derived from pre-existing endosomes. The total number of ferritin granules per synaptic profile did not increase, suggesting that an additional wave of endocytic events did not occur during those 20 s (Extended Data Fig. 6c). Some of the ferritin-filled small vesicles docked to the active zone (Fig. 3a, right panel; Extended Data Fig. 6b, d), suggesting that these vesicles are synaptic vesicles. These results indicate that recently endocytosed membrane passes through endosomes to regenerate synaptic vesicles within about 5–6 s after fusion.

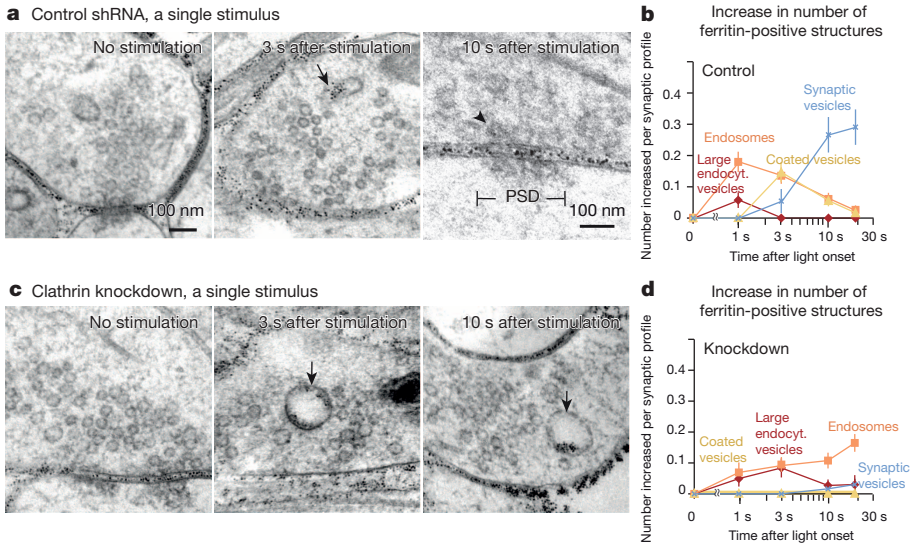

Figure 3 | Following a single stimulus, clathrin is required at endosomes to regenerate synaptic vesicles. **a**, **c**, Electron micrographs showing ferritin uptake in control (**a**) and clathrin knockdown (**c**) synapses at different time points after stimulation. In control neurons, ferritin is observed in large endocytic vesicles after stimulation (middle) and in synaptic vesicles (right), but it is trapped in endosomes in the clathrin knockdown cells. Black arrows indicate ferritin-positive structures. The black arrowhead in **a** represents ferritin-positive synaptic vesicles docked in the active zone. **b**, **d**, Average increase in ferritin-positive endocytic structures in all profiles. **b**, In control cells, the total number of synapses containing ferritin remained at 26% at the 3, 10, and 20 s time points; suggesting that 74% of synapses were silent. The number of synaptic vesicles is higher because after an endosome is resolved it leads to ~2 vesicles that contain a clump of ferritin. The number of clathrin-coated vesicles is less than expected given that endosomes contain 5–8 synaptic vesicles worth of membrane. This discrepancy is probably because synaptic vesicles will be distributed among many thin sections. **d**, In the clathrin knockdown, ferritin stalled in endosomes and did not progress into synaptic vesicles. Clathrin-coated pits were not present on the plasma membrane at any time point and are therefore not plotted. The standard error of the mean is shown in each graph. Experiments are from two independent cultures and at least 149 synaptic profiles were analysed per time point (Supplementary Table 1).

In clathrin knockdown cultures, ferritin-filled endosomes increased after 1 s (Fig. 3d). However, these endosomes did not decline across the 3 s, 10 s or 20 s (Fig. 3c, d). These endosomes formed almost no coated buds and remained spherical (Fig. 3c), suggesting that membrane curvature of the buds requires clathrin. Together, these results suggest that clathrin is required at endosomes to regenerate synaptic vesicles following a single stimulus.

Clathrin at endosomes after 10 stimuli

At mammalian central synapses, action potentials often fire in bursts[16,17] and could exhaust ultrafast endocytosis. To assay endocytosis after high-frequency stimulation, we delivered 10 stimuli (20 Hz for 500 ms in 2 mM Ca^{2+}, 34 °C) and froze cultures 1 s, 3 s, 10 s, and 20 s after the end of the stimulus. Under these conditions, 90% of the cells fired action potentials for all 10 light pulses (Extended Data Fig. 7a). Using cationized ferritin, we followed the fate of the newly endocytosed vesicles (Fig. 4 and Extended Data Fig. 3d, e). The results were similar to those after a single stimulus. Coated pits were not observed on the plasma membrane. Ferritin accumulation in endosomes peaked at 1 s; endosomes exhibited coated buds at 3 s, accompanied by the appearance of clathrin-coated vesicles and some uncoated synaptic vesicles. All vesicles were uncoated by 10 s (Fig. 4a, b and Extended Data Fig. 7b). Ferritin-filled vesicles were eventually recruited to the active zone, suggesting that these vesicles are probably synaptic vesicles (Extended Data Fig. 7c).

We then applied an identical 20 Hz stimulation to cultures treated with clathrin shRNA. In these cultures ferritin was taken up into large endosomes, again suggesting that membrane internalization after a high frequency burst does not require clathrin (Fig. 4c). However, ferritin-containing endosomes were abundant and were not resolved into vesicles even after 20 s (Fig. 4c, d), indicating that clathrin is essential for regenerating vesicles from endosomes after a burst of action potentials. The acute inhibition of clathrin function by Pitstop 2, a potent inhibitor of clathrin-mediated endocytosis, (30 μM, 2 min) also blocked regeneration of synaptic vesicles from endosomes (Extended Data Fig. 8; see Supplementary Information). These results suggest that following a short burst of action potentials, clathrin acts on endosomes to regenerate synaptic vesicles.

To determine whether intense stimulation triggers clathrin-mediated endocytosis, we applied trains of 3, 10, 30, and 100 light pulses at 20 Hz to hippocampal neurons and froze them 10 s after stimulation (2 mM Ca^{2+}, 34 °C). To arrest all endocytic intermediates at the plasma membrane, we applied 80 μM dynasore for 30 s before the stimulation. Dynasore is a drug that binds dynamin[18]; although it also has off-target effects[19], it nevertheless effectively locks both clathrin-mediated endocytosis and ultrafast endocytosis at a late stage of vesicle scission[10,18]. After dynasore treatment, no clathrin-coated pits were trapped on the plasma membrane under any condition. Instead, strings of uncoated vesicles attached to the plasma membrane accumulated at the edges of active zones (Fig. 4e, f). The diameter of vesicles in strings (53.3 ± 3.7 nm) was larger than synaptic vesicles (~40 nm) but smaller than large endocytic vesicles formed after a single stimulus (~80 nm), reflecting reduced fusion during repetitive stimulation. These results suggest ultrafast endocytosis is responsible for removing membrane from the surface even during high frequency bursts of action potentials and that clathrin functions on endosomes rather than at the plasma membrane to regenerate synaptic vesicles.

Ultrafast pathway is temperature sensitive

Actin polymerization is required for ultrafast endocytosis[10]. To study synaptic vesicle recycling in the absence of ultrafast endocytosis, we blocked actin polymerization. We treated cultured neurons with 10 μM latrunculin-A for 30 s, stimulated once by a 10 ms light flash, and frozen 3 or 10 s later (4 mM Ca^{2+}, 34 °C). Large endocytic vesicles adjacent to the active zone were absent following the latrunculin-A application, indicating that ultrafast endocytosis was blocked (Fig. 5a–d). Under these conditions, clathrin-coated pits were observed on the plasma membrane 3 s after stimulation, followed by an accumulation of coated vesicles between 3 and 10 s, and the appearance of large vesicles at 10 s (Fig. 5c, d). The size of coated pits, coated vesicles and synaptic vesicles were similar (Extended Data Fig. 9a).

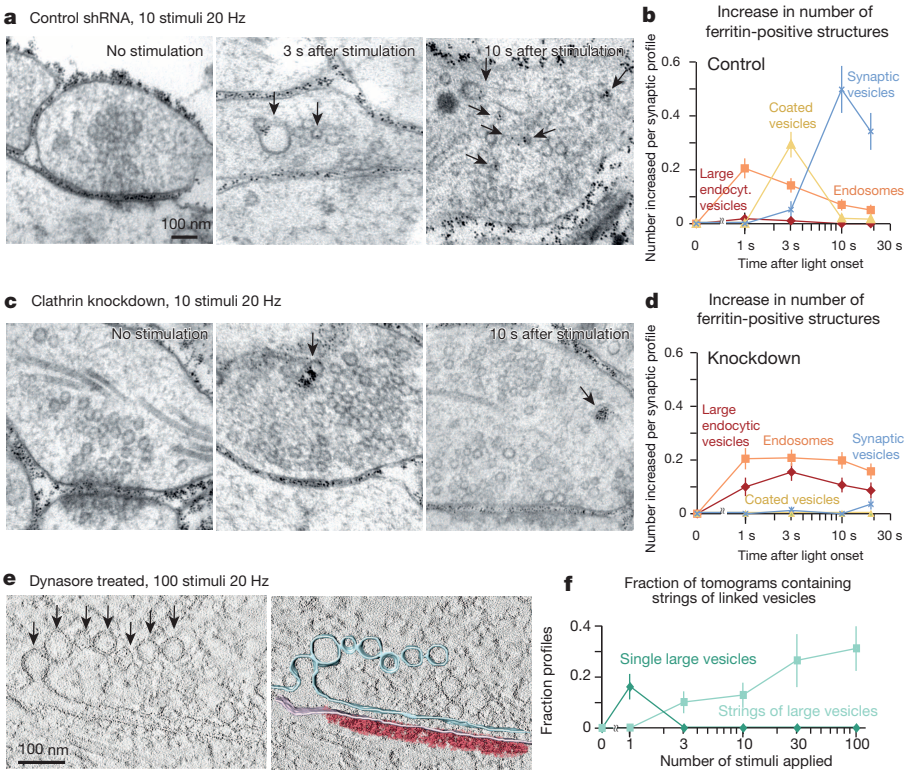

Figure 4 | Following high-frequency stimulation, clathrin is required at endosomes to regenerate synaptic vesicles. **a**, **c**, Electron micrographs showing ferritin uptake in control (**a**) and clathrin knockdown neurons (**c**) at different time points after stimulation. Black arrows indicate ferritin-positive structures. **b**, **d**, Average number of ferritin-positive endocytic structures increased compared to unstimulated cells (0 ms time point) infected with control shRNA (**b**) or clathrin knockdown shRNA (**d**). Clathrin-coated pits were not present on the plasma membrane at any time points and thus not plotted. In the controls, synapses which exhibited ferritin uptake remained at 32%, but the number of ferritin structures per profile increased because endosomes were typically resolved into ~2 ferritin-positive vesicles. Experiments are from two independent cultures and at least 123 synaptic profiles were analyzed per time point (Supplementary Table 1). **e**, Virtual section from an electron tomogram (left) and reconstruction (right) showing a string of large endocytic vesicles trapped on the membrane by dynasore treatment following 100 stimuli at 20 Hz. Multiple large endocytic vesicles (black arrows) are attached to one another and remain connected to the plasma membrane. **f**, Fraction of tomograms that contain vesicle strings attached to the plasma membrane following 1, 3, 10, 30, and 100 stimuli (20 Hz). Tomograms from 100-nm thick sections were reconstructed for each time point; only 1 vesicle string appeared in a given terminal. The number of tomograms with a vesicle string reached 31% following 100 stimuli, suggesting that ~70% of synapses are silent in these preparations. The number of vesicles on a string increases with repetitive stimulation: 1 stimulus (no vesicle string); 3 stimuli (2 vesicles per string); 10 stimuli (2.3 vesicles per string); 30 stimuli (5.6 vesicles per string); and 100 stimuli (4.8 vesicles per string). However, these are probably underestimates because strings that extend into neighbouring sections are not captured in these tomograms. The standard error of the mean is shown in each graph. For *n* values, detailed numbers and statistical analysis, see Supplementary Table 1.

Actin polymerization is known to be less efficient at room temperature in mammalian cells[20,21]. To test whether ultrafast endocytosis fails at low temperature, we incubated cells at room temperature (22 °C) for 5 min before flash-and-freeze (Fig. 5e–h). In control cells maintained at 34 °C, coated pits were not observed after stimulation (Fig. 5e–h, unstimulated, 0/251 synaptic profiles; 3 s, 0/248 synaptic profiles). However, at 22 °C, clathrin-coated pits appeared on the plasma membrane adjacent to the active zone 3 s after a single stimulus (Fig. 5g, h).

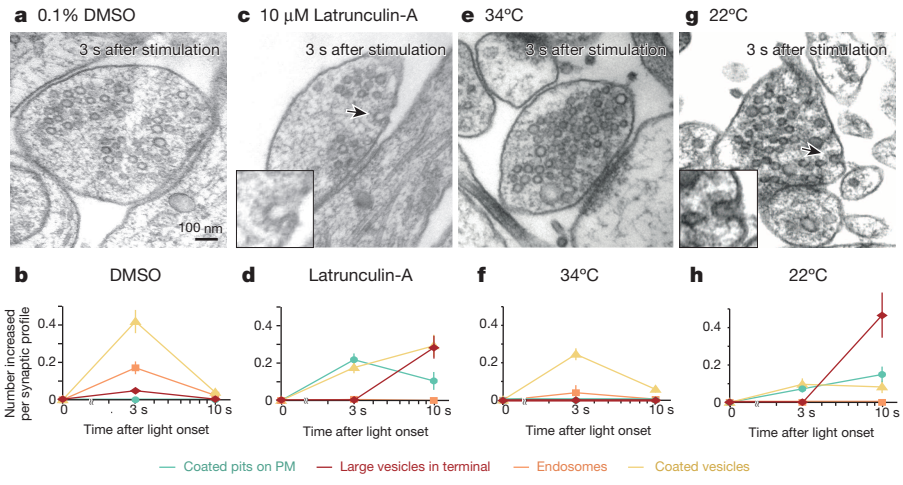

Figure 5 | Clathrin regenerates synaptic vesicles from plasma membrane in the absence of ultrafast endocytosis. **a**, **c**, **e**, **g**, Electron micrographs showing a synaptic terminal 3 s after a single stimulus from cells incubated with 0.1% dimethylsulphoxide (DMSO) (**a**), with 10 µM latrunculin-A (**c**), at 34 °C (**e**), and at 22 °C (**g**). Black arrows indicate clathrin-coated pits. **b**, **d**, **f**, **h**, Average number of endocytic structures per profile in cells incubated with 0.1% DMSO (**b**), 10% latrunculin-A (**d**), at 34 °C (**f**) and at 22 °C (**h**). The total number of structures per profile is plotted. Large vesicles accumulated in the centre of the bouton, probably reflecting the fusion of small endocytic vesicles to endosomes. The standard error of the mean is shown in each graph. Experiments are from two independent cultures and at least 83 synaptic profiles were analysed per time point (Supplementary Table 1).

Like in the latrunculin-A treated cells, large vesicles, possibly endosomes, accumulated in the centre of the bouton 10 s after stimulation[22,23], as observed previously in hippocampal cultures stimulated at room temperature[22,23]. The diameter of coated pits and synaptic vesicles were similar (Extended Data Fig. 9b). These results suggest that failure of ultrafast endocytosis leads to clathrin-mediated endocytosis on the plasma membrane.

Temperature

In classic electron microscopy studies of stimulated synapses, clathrin-mediated endocytosis occurs about 20 s after stimulation[24,25]. By contrast, clathrin-independent ultrafast endocytosis removes excess membrane 30–100 ms after stimulation[10,11], and as demonstrated here, synaptic vesicles are regenerated via an endosome 5–6 s after stimulation (Extended Data Fig. 1). These contradictory results can be reconciled simply by considering temperature.

Ultrafast endocytosis is only observed at physiological temperatures. When neurons are cooled to 22 °C, ultrafast endocytosis fails, and the slower clathrin-mediated process takes over. Actin polymerization is greatly reduced in cultured cells at non-physiological temperature[26,27]. Because ultrafast endocytosis requires actin polymerization, it is probable that vesicle components accumulate on the plasma membrane at room temperature, and the clathrin machinery is recruited to the plasma membrane instead of the synaptic endosome. The shift to clathrin-mediated endocytosis may contribute to rapid synaptic depression that is observed at room temperature[28,29], perhaps because excess membrane in the active zone could block exocytosis.

Previous ultrastructural data have suggested the presence of a fast form of endocytosis at physiological temperature. When frog pectoral muscles were stimulated at 10 °C in the original Heuser and Reese experiments, clathrin-coated pits accumulated on the plasma membrane[1]; whereas when stimulated at room temperature, two forms of endocytosis were observed: a fast form 1 s after stimulation, and a slow form 20 s after stimulation[24]. At snake neuromuscular junctions, clathrin-coated pits accumulated when stimulated at 7 °C[30], whereas at room temperature, membrane was retrieved in 1–2 s[31]. In rat hippocampal neurons, endosomes (> 70 nm) were observed after stimulation at physiological temperature but not at room temperature[32]. Capacitance studies also indicate fast and slow mechanisms. In the calyx of Held, fast endocytosis was observed at physiological temperature (35–37 °C), but was abolished at room temperature[33]. Fast endocytosis was also observed in fish retinal bipolar cells, membrane was recovered ~1 s after a single stimulation[34,35].

Ultrastructure and capacitance analyses only measure membrane endocytosis; protein endocytosis can be measured by pHluorin assays. At room temperature, a slow form of endocytosis is observed in hippocampal neurons with a surface dwell time of 15 s[36]. When pHluorin experiments are conducted at physiological temperatures, the time constant for endocytosis is significantly faster: 14 s at 24 °C and 10 s at 30 °C, and as fast as 6 s at 37 °C[37,38]. At first glance, a 6 s recovery for vesicle proteins agrees well with a 6 s recovery of morphologically defined synaptic vesicles. However, such a comparison is deceptive, as it is unlikely that proteins in a fusing vesicle could diffuse to the lateral edge of the active zone and into an endocytic vesicle within 50 ms. Nevertheless, temperature seems to be responsible for differences observed among ultrastructural studies.

Clathrin at endosomes

Endosomes are sorting compartments that receive cargo from transport vesicles generated by endocytosis from the plasma membrane. Heuser and Reese proposed in their original model that clathrin-mediated endocytosis generated a transport vesicle that fused to an endosome ('cisterna'), and synaptic vesicles were then regenerated from these endosomes[1]. However, subsequent experiments demonstrated that these cisternae were likely to arise via bulk endocytosis due to non-physiological stimulation[25], and the model was amended to propose that synaptic vesicles were generated directly from the plasma membrane via clathrin-mediated endocytosis, whereas bulk endocytosis removed excess membrane added during intense stimulation. Thus, the cisternae do not represent true endosomes as they do not arise via transport vesicles but rather from a simple pinching off from the plasma membrane. Moreover, it was observed that internal clathrin-coated buds were often, or even always, attached to the plasma membrane via long tubules[1,4,39], which led to the idea that the formation of clathrin-coated pits is limited to the plasma membrane. The different lipid compositions of endosomes and the plasma membrane support this notion. Endosomes are enriched for phosphatidylinositol 3-phosphate (PI(3)P), whereas the plasma membrane is enriched in phosphatidylinositol 4,5-bisphosphate ($PI(4,5)P_2$) and therefore can recruit clathrin–AP2 (ref. 40).

By contrast, our data suggest that clathrin regenerates synaptic vesicles from a synaptic endosome rather than from the surface. Tomographic reconstructions of endosomes failed to identify connecting tubules to the plasma membrane. Moreover, these compartments appear to be true endosomes, in that they are generated by transport vesicles. Because endosomes are twice as large as endocytic vesicles, the synaptic endosome probably forms by fusion of endocytic vesicles. The synaptic endosome is resolved into synaptic vesicles by clathrin-mediated budding, and for this reason it is unlikely that synaptic endosome are typical endosomes. The presence of clathrin on these endosomes suggests they are enriched in $PI(4,5)P_2$. In this case, the membrane composition of 'synaptic endosomes' is more like the plasma membrane than that of classical endosomes.

A growing body of molecular studies support the conclusion that synaptic vesicles may be regenerated from endosomes. Live imaging in hippocampal neurons indicates that recently endocytosed vesicle proteins are sorted in an endosome after stimulation[22]. Endosomal Rab GTPases, such as Rab5 and Rab35, are abundant at the synapse and can be co-purified with synaptic vesicles[41], and inhibition of Rab5 (ref. 42) and skywalker[43] (required for Rab35 function) results in an accumulation of endosomes in synaptic boutons. Finally, accumulation of endosomes is also observed in the absence of AP2, clathrin, clathrin accessory proteins or dynamin[44–48].

In summary, our results resolve an important contradiction: most studies indicate that clathrin is essential for endocytosis at hippocampal synapses[36], whereas ultrafast endocytosis is clathrin-independent. Here we demonstrate that even the ultrafast pathway requires clathrin to regenerate synaptic vesicles, not at the plasma membrane but rather at the synaptic endosome. It is probable that at some synapses and under some physiological conditions, clathrin acts at the plasma membrane to regenerate synaptic vesicles. Whether ultrafast endocytosis is a general mechanism or a specialization for synapses with high turnover will require further study.

Online Content Methods, along with any additional Extended Data display items and Source Data, are available in the online version of the paper; references unique to these sections appear only in the online paper.

Received 24 February; accepted 3 September 2014.
Published online 8 October 2014.

1. Heuser, J. E. & Reese, T. S. Evidence for recycling of synaptic vesicle membrane during transmitter release at the frog neuromuscular junction. *J. Cell Biol.* **57,** 315–344 (1973).
2. Maycox, P. R., Link, E., Reetz, A., Morris, S. A. & Jahn, R. Clathrin-coated vesicles in nervous tissue are involved primarily in synaptic vesicle recycling. *J. Cell Biol.* **118,** 1379–1388 (1992).
3. Takei, K. *et al.* Generation of coated intermediates of clathrin-mediated endocytosis on protein-free liposomes. *Cell* **94,** 131–141 (1998).
4. Takei, K., Mundigl, O., Daniell, L. & De Camilli, P. The synaptic vesicle cycle: a single vesicle budding step involving clathrin and dynamin. *J. Cell Biol.* **133,** 1237–1250 (1996).
5. Li, C. *et al.* Ca^{2+}-dependent and -independent activities of neural and non-neural synaptotagmins. *Nature* **375,** 594–599 (1995).
6. Jorgensen, E. M. *et al.* Defective recycling of synaptic vesicles in synaptotagmin mutants of *Caenorhabditis elegans*. *Nature* **378,** 196–199 (1995).
7. Zhang, J. Z., Davletov, B. A., Südhof, T. C. & Anderson, R. G. W. Synaptotagmin I is a high affinity receptor for clathrin AP-2: implications for membrane recycling. *Cell* **78,** 751–760 (1994).

8. Nonet, M. L. *et al.* UNC-11, a *Caenorhabditis elegans* AP180 homologue, regulates the size and protein composition of synaptic vesicles. *Mol. Biol. Cell* **10,** 2343–2360 (1999).
9. Zhang, B. *et al.* Synaptic vesicle size and number are regulated by a clathrin adaptor protein required for endocytosis. *Neuron* **21,** 1465–1475 (1998).
10. Watanabe, S. *et al.* Ultrafast endocytosis at mouse hippocampal synapses. *Nature* **504,** 242–247 (2013).
11. Watanabe, S. *et al.* Ultrafast endocytosis at *Caenorhabditis elegans* neuromuscular junctions. *eLife* **2,** e00723 (2013).
12. Christie, J. M. & Jahr, C. E. Multivesicular release at Schaffer collateral-CA1 hippocampal synapses. *J. Neurosci.* **26,** 210–216 (2006).
13. Berndt, A. *et al.* High-efficiency channelrhodopsins for fast neuronal stimulation at low light levels. *Proc. Natl Acad. Sci. USA* **108,** 7595–7600 (2011).
14. Rizzoli, S. O. *et al.* Evidence for early endosome-like fusion of recently endocytosed synaptic vesicles. *Traffic* **7,** 1163–1176 (2006).
15. Royle, S. J., Bright, N. A. & Lagnado, L. Clathrin is required for the function of the mitotic spindle. *Nature* **434,** 1152–1157 (2005).
16. Lee, D., Lin, B.-J. & Lee, A. K. Hippocampal place fields emerge upon single-cell manipulation of excitability during behavior. *Science* **337,** 849–853 (2012).
17. Sik, A., Penttonen, M., Ylinen, A. & Buzsaki, G. Hippocampal CA1 interneurons: an *in vivo* intracellular labeling study. *J. Neurosci.* **15,** 6651–6665 (1995).
18. Macia, E. *et al.* Dynasore, a cell-permeable inhibitor of dynamin. *Dev. Cell* **10,** 839–850 (2006).
19. Park, R. J. *et al.* Dynamin triple knockout cells reveal off target effects of commonly used dynamin inhibitors. *J. Cell Sci.* **126,** 5305–5312 (2013).
20. Kane, R. E. Actin polymerization and interaction with other proteins in temperature-induced gelation of sea urchin egg extracts. *J. Cell Biol.* **71,** 704–714 (1976).
21. Jensen, V., Walaas, S. I., Hilfiker, S., Ruiz, A. & Hvalby, Ø. A delayed response enhancement during hippocampal presynaptic plasticity in mice. *J. Physiol. (Lond.)* **583,** 129–143 (2007).
22. Hoopmann, P. *et al.* Endosomal sorting of readily releasable synaptic vesicles. *Proc. Natl Acad. Sci. USA* **107,** 19055–19060 (2010).
23. Schikorski, T. Readily releasable vesicles recycle at the active zone of hippocampal synapses. *Proc. Natl Acad. Sci. USA* **111,** 5415–5420 (2014).
24. Miller, T. M. & Heuser, J. E. Endocytosis of synaptic vesicle membrane at the frog neuromuscular junction. *J. Cell Biol.* **98,** 685–698 (1984).
25. Heuser, J. & Reese, T. in *Fourth Intensive Study Program in the Neurosciences* 573–600 (M.I.T. Press, 1979).
26. Gisselsson, L. L., Matus, A. & Wieloch, T. Actin redistribution underlies the sparing effect of mild hypothermia on dendritic spine morphology after *in vitro* ischemia. *J. Cereb. Blood Flow Metab.* **25,** 1346–1355 (2005).
27. Hartmann-Petersen, R., Walmod, P. S., Berezin, A., Berezin, V. & Bock, E. Individual cell motility studied by time-lapse video recording: influence of experimental conditions. *Cytometry* **40,** 260–270 (2000).
28. Pyott, S. J. & Rosenmund, C. The effects of temperature on vesicular supply and release in autaptic cultures of rat and mouse hippocampal neurons. *J. Physiol. (Lond.)* **539,** 523–535 (2002).
29. Kushmerick, C., Renden, R. & von Gersdorff, H. Physiological temperatures reduce the rate of vesicle pool depletion and short-term depression via an acceleration of vesicle recruitment. *J. Neurosci.* **26,** 1366–1377 (2006).
30. Teng, H., Cole, J. C., Roberts, R. L. & Wilkinson, R. S. Endocytic active zones: hot spots for endocytosis in vertebrate neuromuscular terminals. *J. Neurosci.* **19,** 4855–4866 (1999).
31. Teng, H., Lin, M. Y. & Wilkinson, R. S. Macroendocytosis and endosome processing in snake motor boutons. *J. Physiol. (Lond.)* **582,** 243–262 (2007).
32. Micheva, K. D. & Smith, S. J. Strong effects of subphysiological temperature on the function and plasticity of mammalian presynaptic terminals. *J. Neurosci.* **25,** 7481–7488 (2005).
33. Renden, R. & von Gersdorff, H. Synaptic vesicle endocytosis at a CNS nerve terminal: faster kinetics at physiological temperatures and increased endocytotic capacity during maturation. *J. Neurophysiol.* **98,** 3349–3359 (2007).
34. von Gersdorff, H. & Matthews, G. Dynamics of synaptic vesicle fusion and membrane retrieval in synaptic terminals. *Nature* **367,** 735–739 (1994).
35. Neves, G., Gomis, A. & Lagnado, L. Calcium influx selects the fast mode of endocytosis in the synaptic terminal of retinal bipolar cells. *Proc. Natl Acad. Sci. USA* **98,** 15282–15287 (2001).
36. Granseth, B., Odermatt, B., Royle, S. J. & Lagnado, L. Clathrin-mediated endocytosis is the dominant mechanism of vesicle retrieval at hippocampal synapses. *Neuron* **51,** 773–786 (2006).
37. Balaji, J. & Ryan, T. A. Single-vesicle imaging reveals that synaptic vesicle exocytosis and endocytosis are coupled by a single stochastic mode. *Proc. Natl Acad. Sci. USA* **104,** 20576–20581 (2007).
38. Armbruster, M., Messa, M., Ferguson, S. M., De Camilli, P. & Ryan, T. A. Dynamin phosphorylation controls optimization of endocytosis for brief action potential bursts. *eLife* **2,** e00845 (2013).
39. Gad, H., Löw, P., Zotova, E., Brodin, L. & Shupliakov, O. Dissociation between Ca^{2+}-triggered synaptic vesicle exocytosis and clathrin-mediated endocytosis at a central synapse. *Neuron* **21,** 607–616 (1998).
40. Wenk, M. R. & De Camilli, P. Protein–lipid interactions and phosphoinositide metabolism in membrane traffic: insights from vesicle recycling in nerve terminals. *Proc. Natl Acad. Sci. USA* **101,** 8262–8269 (2004).
41. Takamori, S. *et al.* Molecular anatomy of a trafficking organelle. *Cell* **127,** 831–846 (2006).
42. Wucherpfennig, T., Wilsch-Bräuninger, M. & González-Gaitán, M. Role of *Drosophila* Rab5 during endosomal trafficking at the synapse and evoked neurotransmitter release. *J. Cell Biol.* **161,** 609–624 (2003).
43. Uytterhoeven, V., Kuenen, S., Kasprowicz, J., Miskiewicz, K. & Verstreken, P. Loss of skywalker reveals synaptic endosomes as sorting stations for synaptic vesicle proteins. *Cell* **145,** 117–132 (2011).
44. Gu, M. *et al.* AP2 hemicomplexes contribute independently to synaptic vesicle endocytosis. *eLife* **2,** e00190 (2013).
45. Heerssen, H., Fetter, R. D. & Davis, G. W. Clathrin dependence of synaptic-vesicle formation at the *Drosophila* neuromuscular junction. *Curr. Biol.* **18,** 401–409 (2008).
46. Kasprowicz, J. *et al.* Inactivation of clathrin heavy chain inhibits synaptic recycling but allows bulk membrane uptake. *J. Cell Biol.* **182,** 1007–1016 (2008).
47. Kononenko, N. L. *et al.* Clathrin/AP-2 mediate synaptic vesicle reformation from endosome-like vacuoles but are not essential for membrane retrieval at central synapses. *Neuron* **82,** 981–988 (2014).
48. Kittelmann, M. *et al. In vivo* synaptic recovery following optogenetic hyperstimulation. *Proc. Natl Acad. Sci. USA* **110,** E3007–E3016 (2013).

Supplementary Information is available in the online version of the paper.

Acknowledgements We would like to thank D. Lorenz and A. Muenster-Wandowski for providing access to electron microscopy, J. Iwasa for the original model figure, S. Jorgensen for image processing, and C. Garner for discussions. We thank EMBO for providing the travel funds (S.W.). The research was funded by the US National Institutes of Health (NS034307 EMJ), European Research Council grant (249939 SYNVGLUT CR), and German Research Council grants (Neurocure EXC 257 EMJ+CR, SFB 665 + SFB 958 CR). E.M.J. is an Investigator of the Howard Hughes Medical Institute and is an Alexander von Humboldt Scholar.

Author Contributions S.W., C.R., and E.M.J. conceived and designed experiments. S.W. and B.S.-K. performed the freezing experiments. S.W. performed electron microscopy imaging and analysis. T.T. designed shRNA constructs. T.T. and B.B. generated lentivirus and performed biochemistry. T.T. and B.S.-K. performed immunocytochemistry. T.T., M.C.-P., and B.R.R. performed electrophysiology. A.F. prepared cell cultures. M.W.D. designed the stimulation device. S.W., T.T., M.C.-P., B.R.R., C.R., and E.M.J. wrote the manuscript. C.R. and E.M.J. provided funding, experiments were performed at the Charité, Berlin.

Author Information Reprints and permissions information is available at www.nature.com/reprints. The authors declare no competing financial interests. Readers are welcome to comment on the online version of the paper. Correspondence and requests for materials should be addressed to E.M.J. (jorgensen@biology.utah.edu) or C.R. (christian.rosenmund@charite.de).

METHODS

Cell culture and lentivirus infection. Animals were handled according to the rules of the Berlin authorities and the animal welfare committee of the Charité Berlin, Germany. Hippocampi were dissected from newborn C57/BL6-N mice and cultured at 13×10^3 cells per cm^2 on 6 mm sapphire disks for 'flash-and-freeze' electron microscopy experiments and 25 mm coverslips for all other experiments as previously described[10]. Astrocytes were seeded a week in advance to generate a feeder layer. For autaptic cultures, microislands of astrocytes were prepared as previously described[28] and neurons were plated at 300 cells per cm^2. For biochemistry, 10×10^4 cells per cm^2 were cultured without the feeder layer.

Lentivirus was produced as described previously[50]. The cells were infected with lentivirus expressing ChetaTC[10] on DIV1 and clathrin or non-specific shRNA on DIV7. Infection of clathrin shRNA at DIV1 caused severe loss of neurons at DIV14, and thus, cells were only infected for 1 week with clathrin shRNA for all the experiments.

shRNA constructs. A mouse CHC-1 specific siRNA target sequence (5′-GTTG GTGACCGTTGTTATG-3′) was obtained using Genscript siRNA Target Finder (https://www.genscript.com/ssl-bin/app/rnai) and cloned as shRNA into a lentiviral shuttle vector under the control of a U6 promoter. For the scrambled shRNA control sequence we adapted the scrambled siRNA sequence from ref. 15 and cloned it as shRNA (5′-TTCGCACCCTACTTCGTGG-3′) into a lentiviral shuttle vector. Both sequences were subject to a BLAST search to ensure that mouse CHC-1 shRNA was specific and that the scrambled shRNA did not match any sequence. To identify infected cells, the shuttle vector contained a human Synapsin-1 promoter, driving an expression of a nuclear-targeted red fluorescent protein (NLS–RFP).

Western blots and immunocytochemical staining. For detection of clathrin levels by western blots, protein lysates were obtained from astrocyte-free mass cultures of hippocampal neurons. Briefly, cells were lysed using 50 mM Tris/HCl (pH 7.9), 150 mM NaCl, 5 mM EDTA, 1% Triton-X-100, 1% Nonidet P-40, 1% sodium deoxycholate, and protease inhibitors (cOmplete protease inhibitor cocktail tablet, Roche Diagnostics GmbH, Mannheim, Germany). Protein concentration was determined by BCA assay. Proteins were separated by SDS–PAGE and transferred to nitrocellulose membranes. Membranes were then incubated with rabbit anti-CHC-1 (1:500, Abcam, ab21679) and mouse anti-tubulin III (1:2,000, Sigma-Aldrich, T8660) antibodies overnight at 4 °C. After incubation with corresponding horseradish peroxidase-conjugated goat secondary antibodies (1 h at room temperature) and ECL Plus Western Blotting Detection Reagents (GE Healthcare Biosciences), chemiluminescent was imaged using a Vilber Lourmat Fusion FX7 detection system. Ratiometric quantification of signal intensities was measured with the supplied BIO-1D software package of the Fusion FX system. The signals are linear with the amount of protein lysate loaded (data not shown), suggesting that we can detect the clathrin signals in the knockdown without saturating the signals from the control.

Immunocytochemical staining was performed on autaptic cultures. One week after infection with the shRNA constructs, cells were washed once in PBS and fixed with 4% paraformaldehyde (PFA) for 10 min. After washing in PBS, cells were permeabilized with 0.1% PBS-Tween20 for 10 min and blocked in 5% NGS for 30 min. Subsequently cells were incubated with rabbit anti-CHC-1 (1:1,000, abcam, ab21679) and guinea pig anti-synaptophysin (1:1,000, Synaptic System) antibodies overnight at 4 °C. Primary antibodies were labelled with anti-rabbit Alexa Fluor 647 and anti-guinea pig Alexa Fluor 488 (each 1:500, Jackson Immunoresearch Laboratories) for 1 h at room temperature. After washing, coverslips were mounted with Mowiol 4-88 anti-fade medium (Polysciences Europe GmbH, Eppelheim, Germany). Transduced cells, visible by nuclear RFP expression, were imaged using an Olympus IX81 microscope equipped with a Princenton camera and controlled by Metamorph software, with same acquisition settings for all groups. Ratiometric quantification of clathrin signals over synaptophysin signals was conducted in the automated fashion using ImageJ (National Institute of Health, Bethesda, MD) with custom-written macros. In short, the program first subtracts uneven illumination using a 'rolling ball' function with the radius set at 30 pixels (http://fiji.sc/Rolling_Ball_Background_Subtraction). Then, the synapses are defined by thresholding the synaptophysin signals at 15%. The binary image of synaptophysin was used as the regions of interest. The average intensities of fluorescence signals from clathrin heavy chains and synaptopysin were measured from those locations and were divided to obtain ratio between those two proteins. A total of 28 images from the control shRNA cells and 30 images from the clathrin knockdown cells ($n = 2$ cultures) were used.

Electrophysiology. Whole cell patch-clamp and cell-attached voltage-clamp recordings were performed as previously described[10]. The extracellular solution contained 140 mM NaCl, 2.4 mM KCl, 10 mM HEPES, 10 mM Glucose (pH adjusted to 7.3 with NaOH, 300 mOsm). For a single light stimulus experiment, 4 mM $CaCl_2$ and 1 mM $MgCl_2$ were added to the solution, while 2 mM $CaCl_2$ and 1 mM $MgCl_2$ were added for high-frequency stimulation experiments. All recordings were performed at 34 °C.

For recordings in autapses, neurons at DIV15–17 were clamped at −70 mV with a Multiclamp 700B amplifier (Molecular Devices) under control of Clampex 9 (Molecular Devices). The extracellular solution contained 2 mM $CaCl_2$ and 4 mM $MgCl_2$. The patch pipette solution contained 136 mM KCl, 17.8 mM HEPES, 1 mM EGTA, 0.6 mM $MgCl_2$, 4 mM ATP-Mg, 0. 3 mM GTP-Na, 12 mM phosphocreatine and 50 U per ml phosphocreatine kinase (300 mOsm, pH 7.4). EPSCs were evoked by a brief 2 ms somatic depolarization to 0 mV. Readily-releasable pool size was determined by measuring the charge transfer of the transient synaptic current induced by a pulsed 5 s application of hypertonic solution (500 mM sucrose in extracellular solution). Vesicular release probability was calculated as the ratio of the charge from the evoked EPSC (integrated for 1 s) and the readily-releasable pool size.

Electron microscopy. 'Flash-and-freeze' experiments were performed as previously described[10]. Briefly, sapphire disks with cultured cells were mounted in the freezing chamber of the high-pressure freezer (HPM100, Leica), which was set at 34 °C. The temperature 34 °C was chosen to match the temperature of electrophysiological recordings. To minimize the exposure to room temperature, a Petri dish containing the sapphire disk was placed on a 37 °C cryopack while mounting, and the transparent polycarbonate sample cartridges were stored between cyropacks equilibrated to 37 °C. Immediately after the sapphire disk was mounted on the sample holder, recording solution kept at 37 °C was applied to the specimen and the cartridge was inserted into the freezing chamber and allowed to equilibrate to 34 °C for 30 s. For experiments at 37 °C (Extended Data Fig. 2), a temperature-controlled chamber (Leica) was placed around the specimen loading table of the high-pressure freezer. After transferring in a Petri dish, the cells were allowed to recover in the 37 °C chamber for 2 min and then mounted onto the specimen carriers for freezing. The freezing chamber was set at 37 °C in these experiments. Using a home-built light stimulation controller, we applied either 1 or 10 light pulses (20 Hz) to the specimens. The controls for each experiment were always frozen on the same day from the same animal. Each light pulse was for 10 ms. Under these conditions we observe multivesicular release; we estimate that up to 4 synaptic vesicles are released per active zone (data not shown and ref. 10). We set the device so that the samples were frozen at 15, 30, 50, 100, 300, 1,000, 3,000, 10,000 or 20,000 ms after the initiation of the first stimulus[10].

For ferritin-loading experiments, cationized ferritin (Sigma-Aldrich) was added in the recording solution at 0.25 mg ml^{-1}. The calcium concentration was reduced to 1 mM to suppress spontaneous activity during the loading. The cells were incubated in the solution for 5 min at 37 °C. For Pitstop 2 experiments, 30 μM Pitstop 2 was also included in the solution, and the cells were only incubated for 2 min, as longer incubations sometimes yielded dead cells. After ferritin incubation, the cells were immersed in the recording solution containing either 4 mM Ca^{2+} for a single stimulus experiment or 2 mM Ca^{2+} for high-frequency stimulation. The change in calcium concentrations from 1 mM to 4 mM increases the rate of miniature EPSCs and thus may contribute to the background ferritin loading before the experiments. In our experiments, about 1% of synaptic profiles contained endosomes and synaptic vesicles that were ferritin-positive without stimulation. The absence of ferritin-positive coated pits on the plasma membrane in the unstimulated controls suggests that ferritin passes through endosomes even during spontaneous activity. 3 μM NBQX and 30 μM bicuculline were also included in the recording media to minimize the recurrent network activity[10]. Ferritin-positive synaptic vesicles were only found in 5–7% synaptic profiles scored before stimulation using this protocol.

Following high-pressure freezing, samples were transferred into a vial containing 1% osmium tetroxide (EMS), 1% glutaraldehyde (EMS), 1% milliQ water, in anhydrous acetone (EMS). The freeze-substitution was performed in AFS2 (Leica) with the following program: −90 °C for 5–7 h, 5 °C per hour to −20 °C, 12 h at −20 °C, and 10 °C per hour to 20 °C. Following en bloc staining with 0.1% uranyl acetate, the samples were infiltrated and embedded into epon and cured for 48 h in a 60 °C oven. Serial 40-nm sections were cut using a microtome (Leica UCT) and collected onto formvar-coated single-slot grids. Sections were stained with 2.5% uranyl acetate before imaging. For ferritin experiments, sections were not stained after sectioning to improve contrast of ferritin molecules in our images—this, in turn, might have compromised our ability to distinguish clathrin-coated vesicles. Approximately 150 synaptic profiles were collected from a single section from each specimen, and the experiments were repeated with second cultures in each case (for detailed n values, see Supplementary Table 1). The sample size was chosen based on the previous experiments that allowed us to acquire a sufficiently large set of data for statistical analysis[10]. The total numbers of synaptic profiles and tomograms analysed for these experiments are 10,514 and 361, respectively. Note that there is some variability from experiment to experiment; this is probably due to the short lifetimes of these structures. The synaptic profiles were chosen randomly to sample unbiased populations. Active zones were defined as regions juxtaposed to a postsynaptic density. Docked vesicles are defined as those directly in contact with membrane. The large endocytic vesicles are defined as vesicles larger than ~50 nm by visual inspection and within 50 nm of active zone, measured in ImageJ. Endosomes

are defined as membrane-bound organelles that are in the centre of the bouton and larger than 100 nm by visual inspection. Vesicular compartments with coated buds were also categorized as endosomes, which appeared frequently in our 3 s time points. Vesicles are scored as clathrin-coated only if distinctive coats were visible which can lead to underscoring (Fig. 1c and Extended Data Fig. 2c). Furthermore, the chance of capturing a coated vesicle in a given synaptic profile is low compared to an endosome due to its size. These factors will lead to an underestimate of the number of coated vesicles observed in profiles. The morphometry was performed blind using custom-written ImageJ macro and Matlab scripts (Watanabe, Davis, and Jorgensen).

For electron tomography, 100–200 nm thick sections were collected on pioloform-coated single-slot grids. Sections were post-stained with uranyl acetate as described for thin sections. 10-nm gold particles were sparsely applied to both sides of the grids by incubating the grids in drops of solution containing 5.7×10^{12} particles per ml (http://microspheres-nanospheres.com/) for 2 min. 17–50 tilt-series ($\pm 65^{\circ}$) were collected from each sample using FEI TF20 electron microscope. For serial tomograms, low magnification images acquired from each section on a grid were used to locate the same synapses in the serial sections. Typically, the entire synapses span 4 to 5 sections, when cut at 200 nm. The tomograms were generated from tilt-series using IMOD. The tomograms were segmented and reconstructed using Amira or TrakEM2.

Membrane calculations. The amount of membrane on large endocytic vesicles and endosomes was calculated to determine the number of synaptic vesicle equivalents contained in these structures. These structures were scored blind and were distinguished by position in the bouton, by size, and by shape. For large endocytic vesicles in single stimulus experiments (Fig. 1), the mean diameter was 80.6 ± 1.5 nm. The surface area of the large endocytic vesicles is therefore about 20,000 nm^2, as the surface area of a synaptic vesicle is 5,300 nm^2, large endocytic vesicles correspond to 4 synaptic vesicle equivalents. In the RNA interference experiments after a single stimulus, the size of large endocytic vesicles was 82.6 ± 4.5 nm (4 synaptic vesicle equivalents) in the control and 74.4 ± 2.0 nm (3 synaptic vesicle equivalents) in the clathrin knockdown. In the RNA interference experiments after high-frequency stimulation, the size of large endocytic vesicles was 85.5 ± 2.2 nm (4 synaptic vesicle equivalents) in the control and 70.1 ± 1.4 nm (3 synaptic vesicle equivalents) in the knockdown.

The surface area of endosomes was calculated by measuring the diameter and assuming a spherical shape. This calculation will lead to an underestimate of the surface area of endosomes because the membrane in budding endosomes is convoluted. To minimize this error, endosomes with coated buds were not included in the calculations. After a single stimulus (Fig. 1), the mean diameter of endosomes was 116.4 ± 3.0 nm (8 synaptic vesicle equivalents). In the ferritin experiments with a single stimulus, the diameter of endosomes was 108.7 ± 4.2 nm (7 synaptic vesicle equivalents) in the control and 93.1 ± 2.8 nm (5 synaptic vesicle equivalents) in the clathrin knockdown. In the ferritin experiments with multiple stimuli, the diameter of endosomes was 111.8 ± 4.1 nm (8 synaptic vesicle equivalents) in the control and 100.9 ± 2.6 nm (6.5 synaptic vesicle equivalents) in the clathrin knockdown. The smaller size of endocytic structures in the clathrin knockdowns is probably due to the reduced neurotransmission in these cells. To confirm the estimates of surface area, we measured the surface area of complete endosomes in tomograms of wild-type synapses. Most endosomes were spherical with the diameter of 111.2 ± 5.3 nm (39,000 nm^2 or 7.3 synaptic vesicle equivalents). The surface area of budded endosomes was measured to be ~41,000 nm^2 or 7.7 synaptic vesicle equivalents.

Statistics. For detailed numbers and statistical analysis, see Supplementary Table 1.

49. von Kleist, L. *et al.* Role of the clathrin terminal domain in regulating coated pit dynamics revealed by small molecule inhibition. *Cell* **146,** 471–484 (2011).
50. Lois, C., Hong, E. J., Pease, S., Brown, E. J. & Baltimore, D. Germline transmission and tissue-specific expression of transgenes delivered by lentiviral vectors. *Science* **295,** 868–872 (2002).

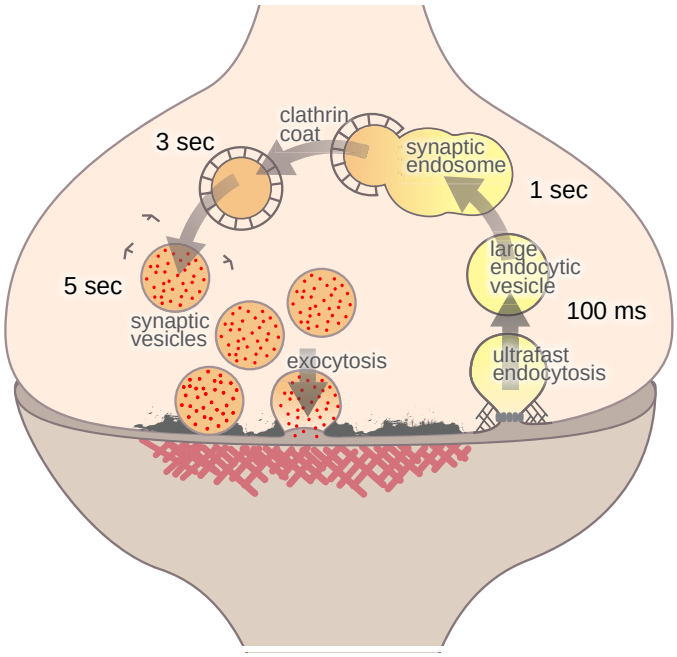

Extended Data Figure 1 | Ultrafast endocytosis regenerates synaptic vesicles in a two-step process. Ultrafast endocytosis removes membrane added by vesicle fusion at the lateral edge of the active zone. Large endocytic vesicles then fuse to endosomes. Endosomes are resolved into synaptic vesicles via a clathrin-dependent process. Newly formed synaptic vesicles can be recruited back to the active zone.

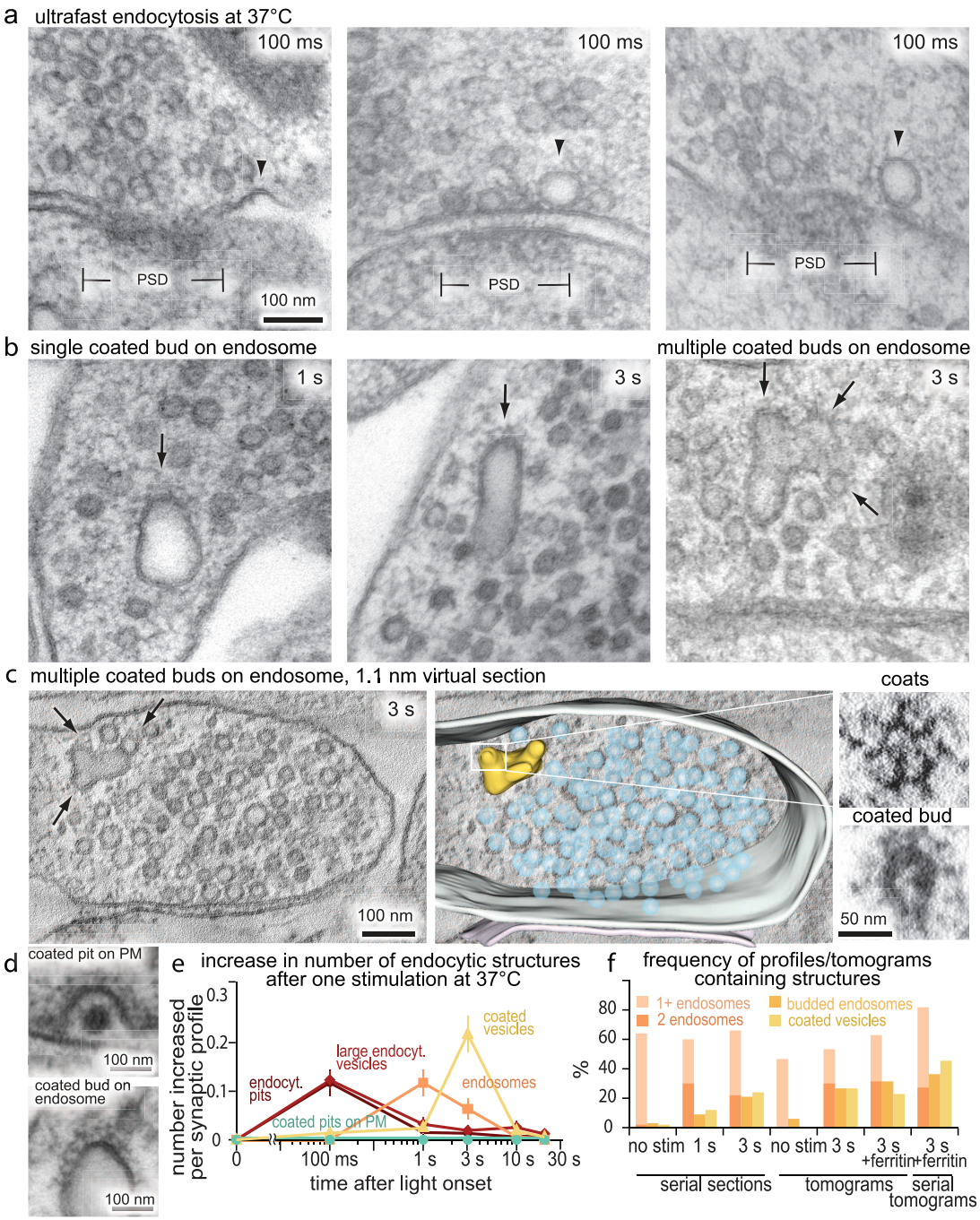

Extended Data Figure 2 | Synaptic vesicles are regenerated from endosomes at 37 °C. Hippocampal synapses were stimulated once and frozen at the indicated times. The experiments were performed at 37 °C in the presence of 4 mM external Ca^{2+}. **a**, Electron micrographs showing invaginations and large endocytic vesicles (arrowheads) recovered via ultrafast endocytosis. **b**, Micrographs showing single coated buds (left, middle) or multiple buds (right) forming on an endosome. Arrows indicate coated buds on an endosome. **c**, Virtual section from an electron tomogram (left) and reconstruction (middle) showing a synaptic endosome with buds following a single stimulus. Arrows indicate coated buds on an endosome. The average intensity of coated buds from the top 20 nm (right, top) and the bottom 40 nm (right, bottom) is shown. Clathrin-cages can be preserved in our fixation and are visible in the tomogram. We found a total of 32 endosomes in these reconstructions (14 endosomes in the unstimulated control and 28 endosomes 3 s after stimulation). Of the total 32 endosomes, none were connected to the plasma membrane or showed evidence of a truncated tubule extending from the endosomal membrane. Of the 14 unstimulated endosomes, 8 were contained within single tomograms, and are therefore unambiguously closed on both ends. Of the 28 endosomes in stimulated synapses, 16 endosomes were contained within single tomograms so that it was clear that no attachment to the plasma membrane was possible. **d**, Examples of a coated pit on the plasma membrane (top) and a coated bud on an endosome (bottom). Note that the morphology of the coats is similar. **e**, Increase in the number of each endocytic structure per synaptic profile after a single stimulus at 37 °C. The prevalence of large endocytic vesicles and endosomes is followed by an increase in the number of clathrin-coated vesicles. Coated pits were not observed on the plasma membrane (PM). **f**, Frequency of profiles or tomograms that contain endosomal structures at 37 °C. Approximately 60% of unstimulated synapses contained one endosome. One second after stimulation, 60% of the synapses contained at least one endosome, and half of those synapses contained two endosomes. Three seconds after stimulation, ~30% of the synapses contained budded endosomes and clathrin-coated vesicles, suggesting that those synapses were active. The standard error of the mean is shown in each graph. At least 146 synaptic profiles were analysed from each time point. For *n* values, detailed numbers and statistical analysis, see Supplementary Table 1.

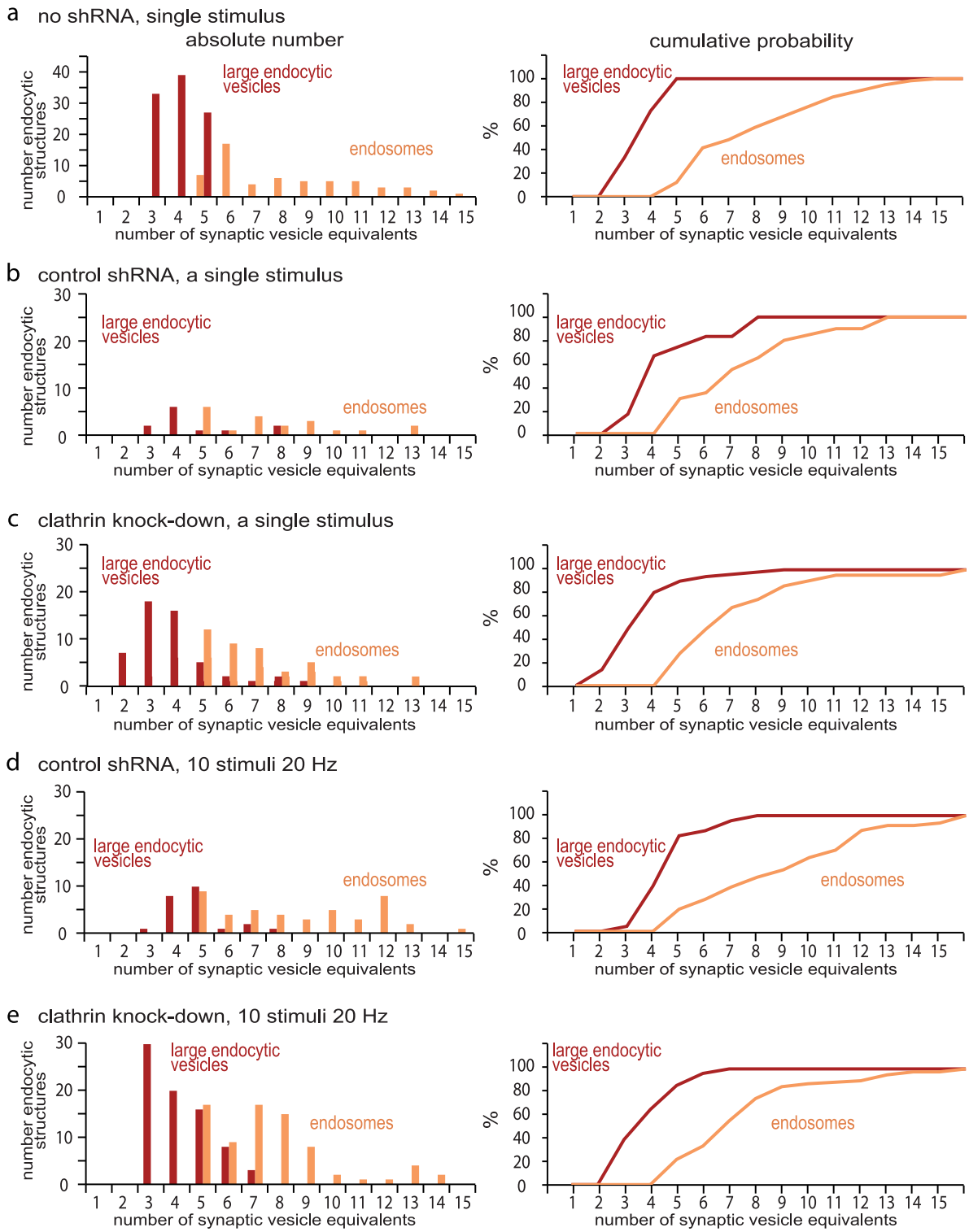

Extended Data Figure 3 | Large endocytic vesicles likely fuse to become synaptic endosomes. **a–e,** Histograms (left) and cumulative plots (right), showing the size of large endocytic vesicles (red) and endosomes (orange) after one stimulus from control cells without ferritin (**a**), scrambled shRNA infected cells (**b**), and clathrin knockdown cells (**c**) both with ferritin. Ten stimuli were applied to scrambled shRNA (**d**) or clathrin knockdown cells (**e**). The large endocytic vesicles are defined as those that are within 50 nm of active zone and larger than a synaptic vesicle by visual inspection. Endosomes are defined as large vesicles greater than 50 nm from the active zone (often in the centre of the bouton) and are larger than ~100 nm. Any vesicular compartment that has coated buds in the centre of the bouton is also categorized as an endosome. The numbers of endocytic structures in (**a**) represent all the structures scored from 100 ms and 300 ms time points. The number of large vesicles and endosomes in **b**–**e** represent all the ferritin-positive structures from later time points (3, 10, and 20 s). In the control shRNA (**b**), the number of large endocytic vesicles and endosomes has declined by these late time points, whereas the ferritin is trapped in large endocytic vesicles and synaptic endosomes in the clathrin knockdown experiments. Because ferritin passes from large endocytic vesicles to even larger budded endosomes, it is probable that the endocytic vesicles fuse with either each other or an existing compartment.

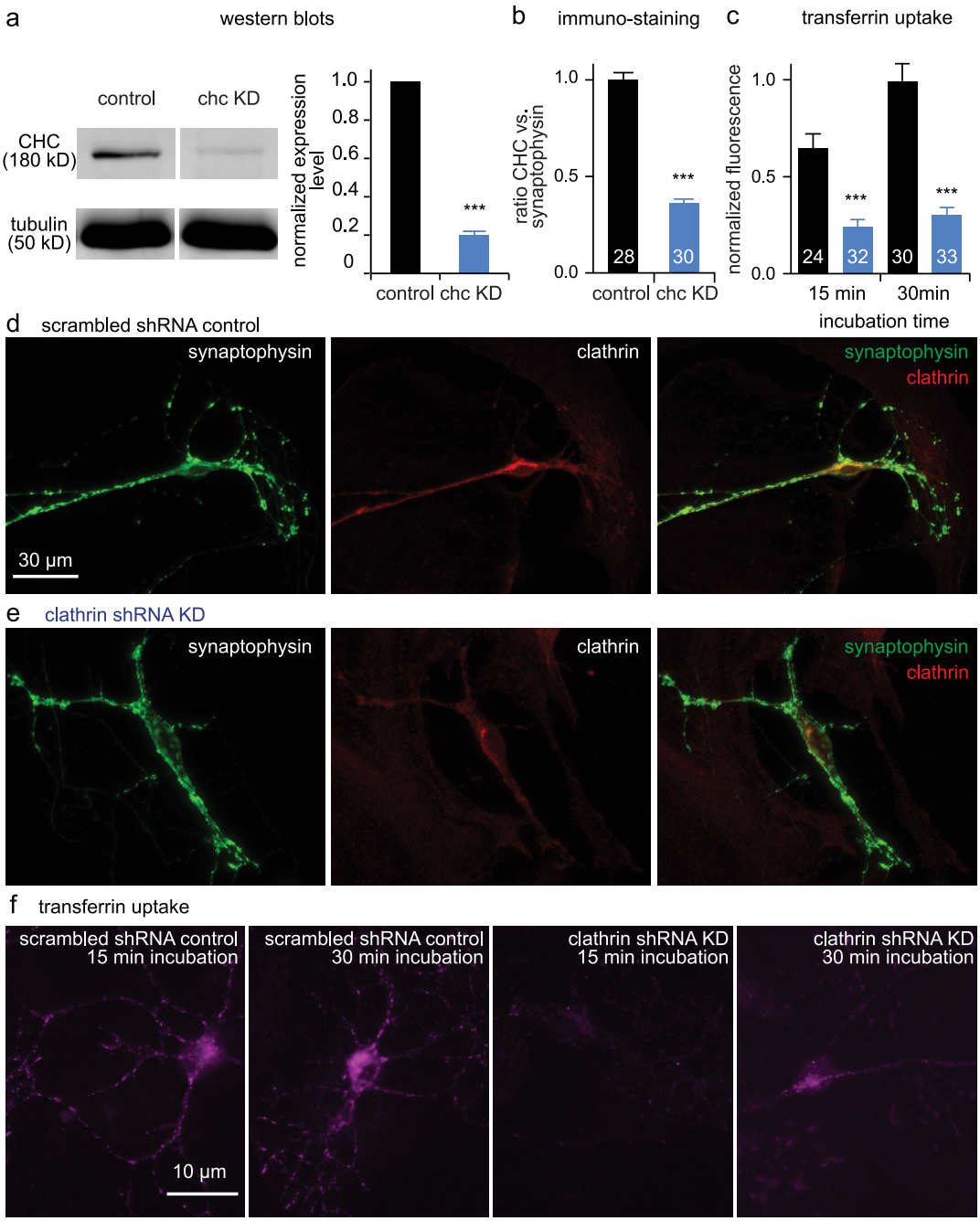

Extended Data Figure 4 | Clathrin shRNA reduces clathrin expression. **a**, Left, western blot showing clathrin levels after one-week expression of a scrambled shRNA control or clathrin heavy chain shRNA in cultured hippocampal neurons. Right, an 80% reduction was observed ($n = 3$, $P < 0.001$, paired t-test). **b**, Normalized ratio of clathrin heavy chain and synaptophysin fluorescence in control and clathrin knockdown (chc KD) cultures. The clathrin/synaptophysin ratio is reduced to 64% in the knockdown cells. **c**, The mean fluorescence intensity (normalized to 30 min) representing the amount of transferrin uptake in control and knockdown cells. Transferrin uptake was reduced by 66% in the knockdown cells. **d**, **e**, Fluorescence images of immunocytochemical staining of hippocampal autaptic cultures using anti-synaptophysin (left), anti-clathrin heavy chain (middle), and merge in control (**d**) and clathrin knockdown cultures (**e**). **f**, Example micrographs of hippocampal mass cultures showing transferrin uptake. The standard error of the mean is shown. ***$P < 0.001$. For detailed numbers and statistical analysis, see Supplementary Table 1.

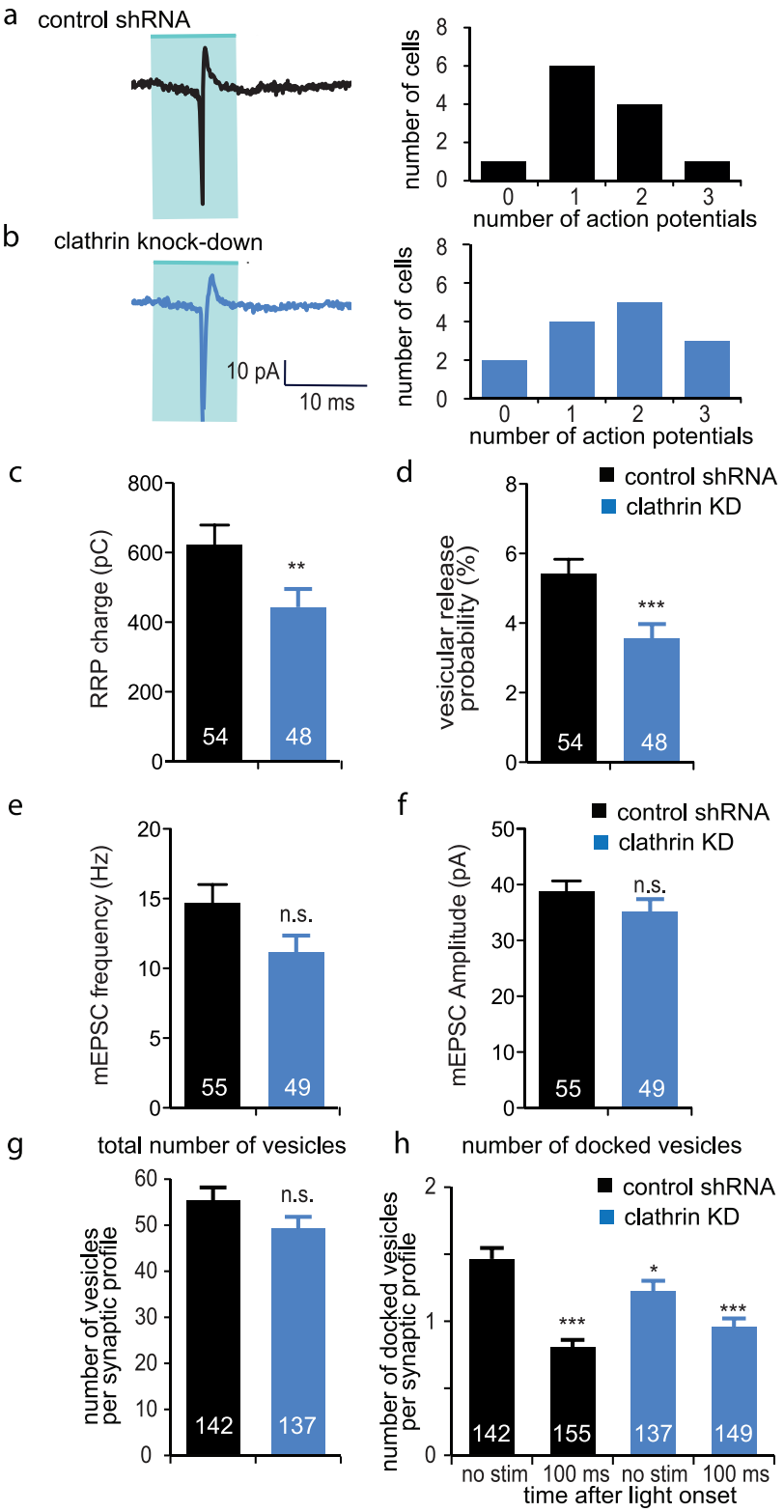

Extended Data Figure 5 | Exocytic machinery is intact in the clathrin knockdown cells. **a**, **b**, Sample traces from cell-attached voltage clamp during light stimulation in control (**a**) and clathrin knockdown (**b**). Number of action potentials triggered during the 10 ms light pulse is shown to the right. **c**, Readily-releasable pool (RRP) in control and clathrin knockdown cells, defined by brief application of 500 mM sucrose to autaptic neurons (control: 622 ± 56 pC, knockdown: 443 ± 52 pC, $P < 0.01$). **d**, Vesicular release probability (Pvr) in these cells (control 5.4 ± 0.4%, $n = 54$; knockdown 3.5 ± 0.4%, $n = 48$; $P < 0.001$). **e**, **f**, Average miniature EPSC (mEPSC) frequency (**e**) and amplitude (**f**). No change was observed in knockdown cells. **g**, Average number of synaptic vesicles per synaptic profile ($n = 142$ synapses for control and 137 for knockdown). **h**, Average number of docked vesicles in active zones per synaptic profile (control: no stimulation, 1.5 ± 0.1, $n = 142$ synapses; 100 ms, 0.8 ± 0.1, $n = 142$ synapses; knockdown: no stimulation, 1.2 ± 0.1, $n = 137$ synapses; 100 ms after stimulation, 1.0 ± 0.1, $n = 149$ synapses). The fraction of docked vesicles that fuse is greatly reduced by clathrin knockdown. P values are calculated against the unstimulated control shRNA cells. The standard error of the mean is shown in each graph. ***$P < 0.001$, **$P < 0.01$, and *$P < 0.05$, respectively. n.s., not significant.

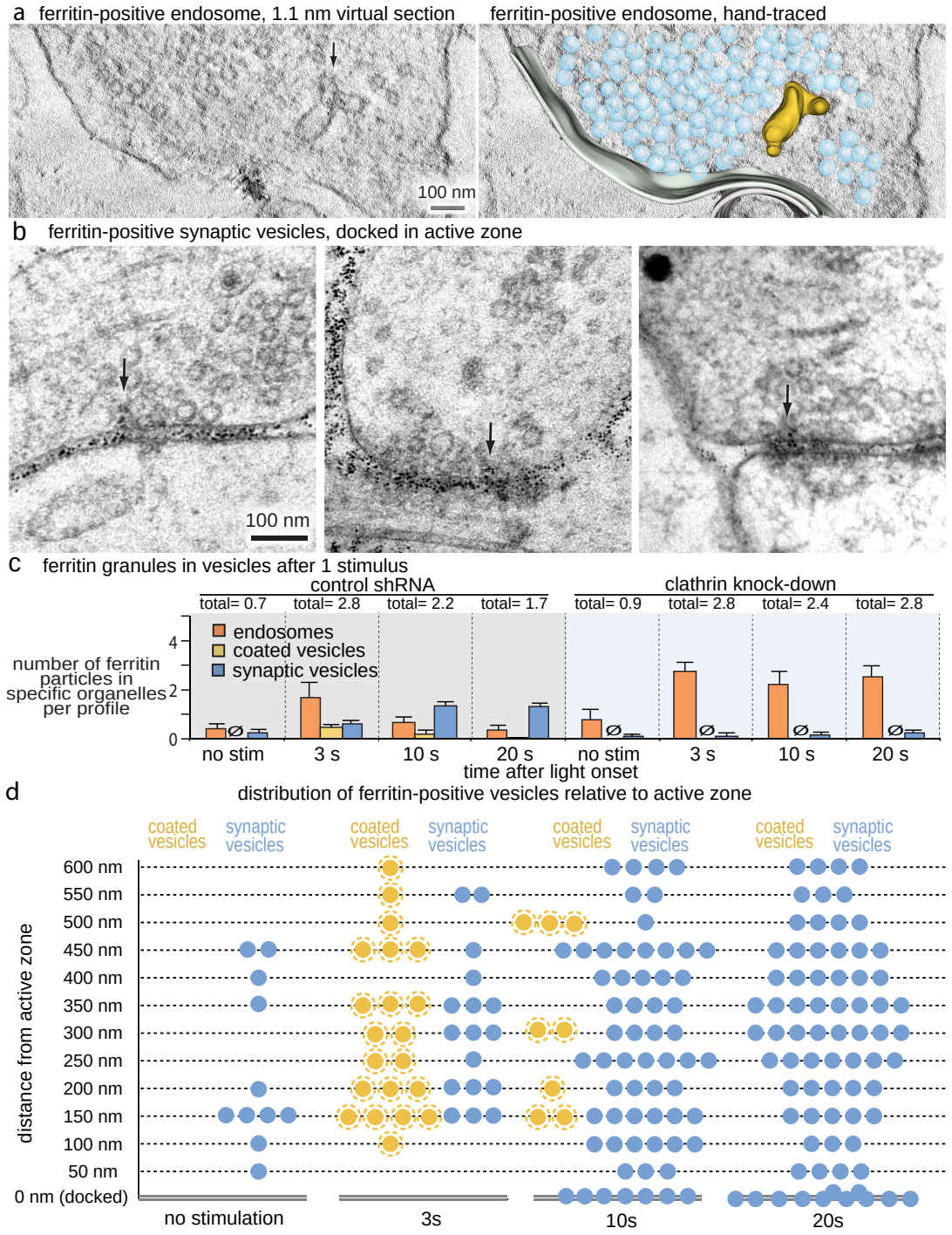

Extended Data Figure 6 | Following a single stimulus, clathrin is required at endosomes to regenerate synaptic vesicles. a, Virtual section from an electron tomogram (left) and a reconstruction (right) showing a budded synaptic endosome containing ferritin particles in the scrambled shRNA control cell. We found a total of 33 endosomes in these reconstructions. Of these 33 endosomes, none were connected to the plasma membrane or showed evidence of a tubule extending from the endosomal membrane. A total of 17 of these 33 total endosomes were fully contained within the 200 nm tomogram. Of these 33 endosomes, 16 were ferritin-positive, and 8 of these 16 endosomes were fully contained in the tomogram. **b**, Micrographs showing ferritin-positive synaptic vesicles docked to active zone 10–20 s after stimulation. **c**, Average number of ferritin particles in large endocytic vesicles, clathrin-coated vesicles, and synaptic vesicles per synaptic profile examined. At least 134 synapses were analysed per time point. Ferritin progresses to synaptic vesicles in the control, but is trapped in large endocytic vesicles or endosomes in the clathrin knockdown. The fraction of synaptic profiles with ferritin was 27% for the control and 31% in the knockdown, suggesting that 70% of the synapses were silent. The mean number of ferritin particles found in an individual endosome, clathrin-coated vesicle, and synaptic vesicle, are 9.3 ± 1.0, 2.0 ± 0.2, and 1.9 ± 0.2, respectively. The total number of ferritin particles (indicated above), declined by 40% in the control relative to the 1 s time point but not in the knockdown, either due to the fusion of the newly formed synaptic vesicles or by return of excess membrane to the surface of the synapse. The standard error of the mean is shown. **d**, Distribution of ferritin-positive clathrin-coated vesicles (yellow) and synaptic vesicles (blue) relative to the active zone at defined time points after stimulation in the control cells. Numbers are binned by 50 nm. The first bin '0 nm' means vesicles are docked in active zone. Endosomes are found at 285 ± 38 nm from the active zone. Note that the data in this figure represent further analysis of the data shown in Fig. 3.

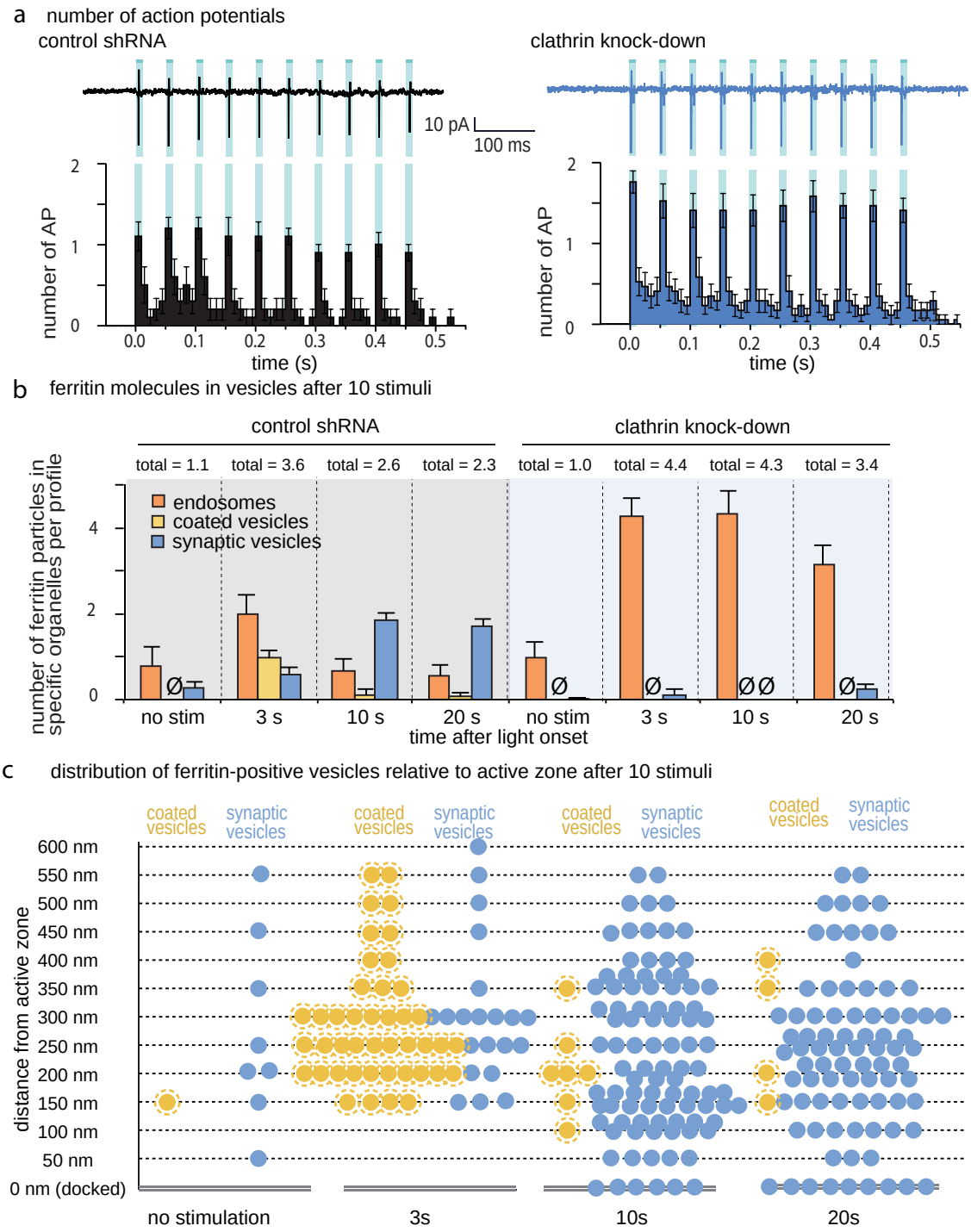

Extended Data Figure 7 | Following high-frequency stimulation, clathrin is required at endosomes to regenerate synaptic vesicles. a, Average number of action potentials in 10 ms bins relative to light pulses during high-frequency stimulation (10 stimuli at 20 Hz, 0.5 s). Sample traces are shown above. Each light pulse triggered at least one action potential in both control and clathrin shRNA-treated cultures. **b**, Average number of ferritin molecules in large endocytic vesicles, clathrin-coated vesicles, and synaptic vesicles per profile examined. Ferritin is transferred from large endocytic vesicles to synaptic vesicles in the control but is trapped in large endocytic vesicles or endosomes in the clathrin knockdown. The number of profiles with ferritin particles after stimulation was 34% in the control and 36% in the clathrin knockdown, suggesting that 65% of the synapses were silent. On average, the number of ferritin molecules found in an individual endosome, clathrin-coated vesicle, and synaptic vesicle, are 9.2 ± 1.0, 1.9 ± 0.3, and 2.0 ± 0.2. At least 142 synapses were analysed per time point. The total number of ferritin particles (indicated above each time point), declined by 36% in the control, and by 23% in the knockdown relative to the 1 s time point. **c**, Distribution of ferritin-positive clathrin-coated vesicles (yellow) and synaptic vesicles (blue) relative to the active zone at defined time points after stimulation in the control shRNA cells. Numbers are binned by 50 nm. The first bin '0 nm' means vesicles are docked at the active zone. Endosomes are found at 286 ± 43 nm from the active zone. The standard error of the mean is shown in each graph. Note that this figure represents further analysis of the data from Fig. 4.

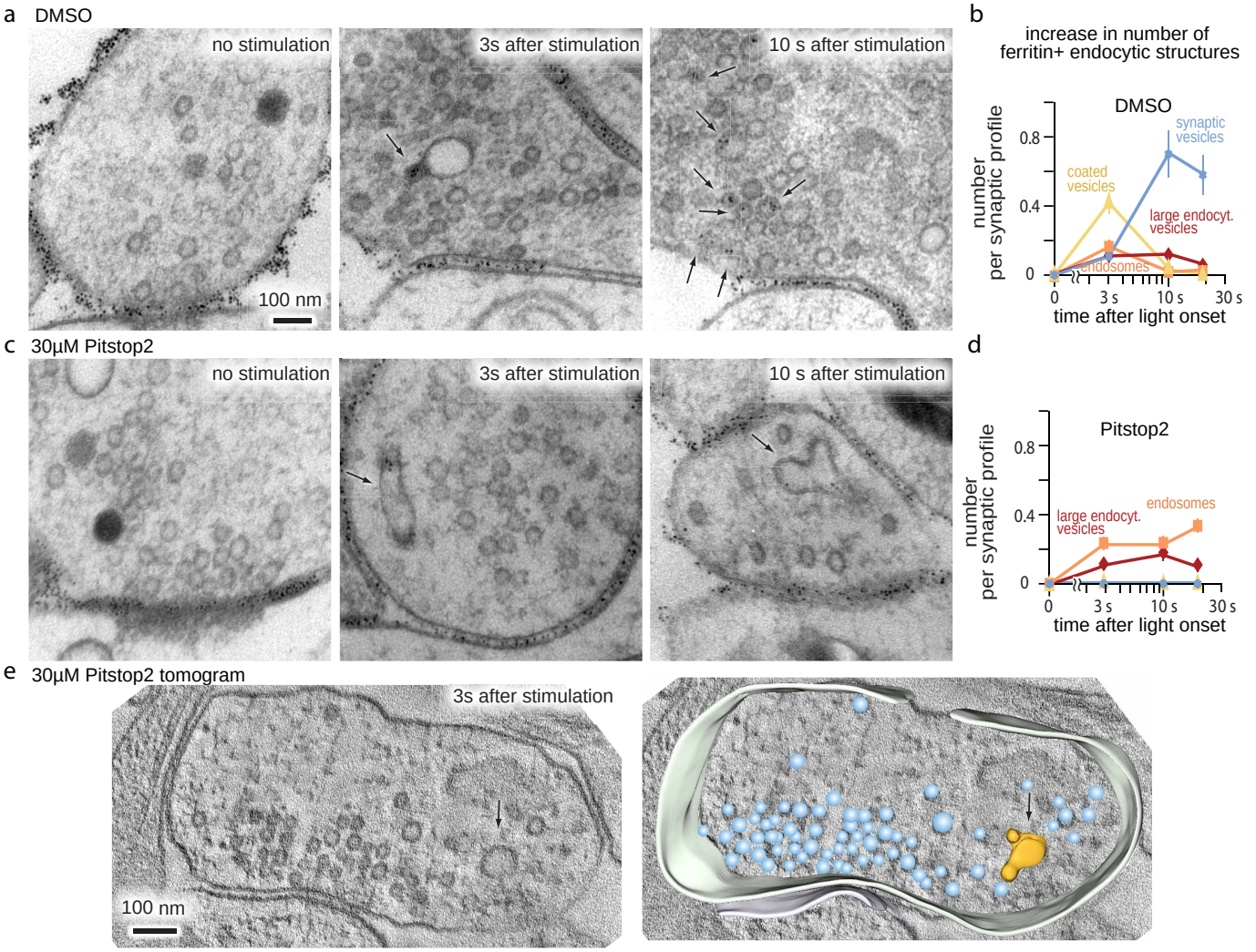

Extended Data Figure 8 | Pitstop 2 blocks regeneration of synaptic vesicles from endosomes after high-frequency stimulation. Pitstop 2 is an inhibitor of clathrin terminal domain and blocks clathrin-mediated endocytosis[49]. **a**, **c**, Electron micrographs showing ferritin containing vesicles in DMSO-treated (**a**) and Pitstop-2-treated cells (**c**) at different time points after stimulation. Ferritin is found in large vesicles after stimulation (middle) and in synaptic vesicles (right) in control, but it is trapped in endosomes in the Pitstop-2-treated cells. **b**, **d**, Average increase in ferritin-positive structures per synaptic profile in DMSO-treated (**b**) or Pitstop-2-treated cells (**d**). Ferritin progressed to synaptic vesicle-like structures in the control but remained in endosomes or large endocytic vesicles in Pitstop-2-treated cells. Clathrin-coated pits on the plasma membrane were not present at any time point and were not plotted. At least 140 synapses were analysed per time point. **e**, Virtual section from an electron tomogram (left) and a reconstruction (right) showing a synaptic endosome with buds following 10 stimuli at 20 Hz. Of 32 tomograms reconstructed from the 3 s time point, 25 of them showed at least one endosome in the terminal, and 7 showed budded endosomes. None of these endosomes were connected to the plasma membrane. The standard error of the mean is shown in each graph. For detailed numbers and statistical analysis, see Supplementary Table 1.

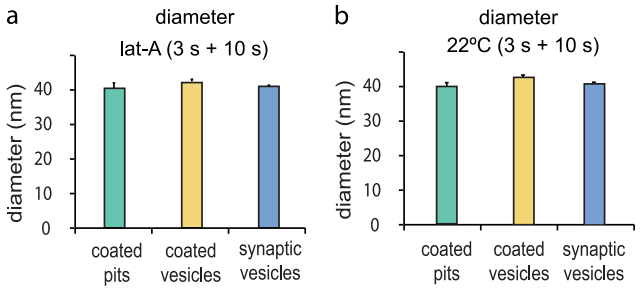

Extended Data Figure 9 | Synaptic vesicles are regenerated directly from the plasma membrane in the absence of ultrafast endocytosis. **a**, **b**, Average diameter of clathrin-coated pits, clathrin-coated vesicles, and synaptic vesicles in the latrunculin-A treated cells (**a**) or cells incubated at 22 °C for 5 min (**b**). The diameter of these structures is similar suggesting a precursor–product relationship. Diameter of coated pits was determined by the full-width at the half maximum depth of the pit. For detailed numbers and statistical analysis, see Supplementary Table 1.